Weierstraß-Institut
für Angewandte Analysis und Stochastik
Leibniz-Institut im Forschungsverbund Berlin e. V.

Preprint ISSN 0946 – 8633

Directionality of THz emission from photoinduced gas plasmas

Christian Köhler[1], Eduardo Cabrera-Granado[1], Ihar Babushkin[2], Luc Bergé[3],
Joachim Herrmann[4], Stefan Skupin[1,5],

submitted: 30 Jun 2011

[1] Max Planck Institute
for the Physics of
Complex Systems
Nöthnitzer Str. 38
01187 Dresden
Germany

[2] Weierstrass Institute
Mohrenstr. 39
10117 Berlin
Germany
E-mail: ihar.babushkin@wias-berlin.de

[3] CEA-DAM, DIF
F-91297 Arpajon
France

[4] Max Born Institute
for Nonlinear Optics
and Short Time
Spectroscopy
Max-Born-Str. 2A
12489 Berlin
Germany

[5] Friedrich Schiller University
Institute of Condensed Matter
Theory and Optics
Fröbelstieg 1
07742 Jena
Germany

No. 1627
Berlin 2011

2010 *Mathematics Subject Classification.* 35Q60, 78A60, 76X05.

Key words and phrases. THz emission, photoinduced plasma, nonlinear optics.

Edited by
Weierstraß-Institut für Angewandte Analysis und Stochastik (WIAS)
Leibniz-Institut im Forschungsverbund Berlin e. V.
Mohrenstraße 39
10117 Berlin
Germany

Fax: +49 30 2044975
E-Mail: `preprint@wias-berlin.de`
World Wide Web: `http://www.wias-berlin.de/`

Abstract

Forward and backward THz emission by ionizing two-color laser pulses in gas is investigated by means of a simple semi-analytical model based on Jefimenko's equation and rigorous Maxwell simulations in one and two dimensions. We find the emission in backward direction having a much smaller spectral bandwidth than in forward direction and explain this by interference effects. Forward THz radiation is generated predominantly at the ionization front and is thus almost not affected by the opacity of the plasma, in excellent agreement with results obtained from a unidirectional pulse propagation model.

Generation of radiation in the THz range and controlling its spectrum and direction of emission is crucial for applications reaching from nonlinear THz spectroscopy to biomedical and security imaging. Several methods for THz generation, such as photoconductive switches or optical rectification in second order nonlinear crystals are limited in achievable THz field amplitudes due to saturation or material damage for high input intensities. An alternative setup [1–6], where an ionizing two-color laser pulse is focused into a gas cell has attracted much interest, since the obtained THz pulses are characterized by comparably high amplitudes and broad spectra. The THz emission can be explained by a low frequency component in the plasma current caused by the asymmetric two-color laser field [2], where the stepwise modulation of the electron current by two-color tunneling ionization plays a crucial role [6]. Within this model, good agreement of forward (FW) emitted THz radiation in experiment and simulation was obtained recently [6]. In contrast to studies on THz generation mediated by ponderomotive and relativistic effects in plasmas [7], an investigation of possible backward (BW) THz emission due to the above mentioned mechanism is still missing.

In this Letter we present a combined analytical and numerical study of THz generation by ionizing two-color femtosecond pulses in a gas. We reveal the governing effect for differences in FW and BW emitted THz spectra to be interference of signals from different spatial positions in the plasma channel. Furthermore, we find that opacity of the plasma is of minor influence on FW THz emission in focused pump geometries.

Let us first develop a simple picture to explain the main difference between FW and BW emitted fields. A simplified though generic setup is shown in Fig. 1. We assume a plasma line-source of length L on the z-axis, which is meant to be produced by a laser pulse propagating in positive z-direction (FW). At each point, the pump pulse ionizes the medium, the generated free electrons are accelerated in the laser field and thus build up a current $J_e(t)$, which in turn emits electromagnetic radiation. Due to the propagation of the ionizing pump pulse, points with smaller z-coordinates emit radiation earlier than the ones with larger z-coordinates. If all propagation effects (diffraction, dispersion, etc.) are neglected, the pulse moves unchanged and all constituent points along the plasma line emit the same field, but shifted in time. This is illustrated in Fig. 1(a), where a snapshot of the emitting plasma line is shown. Each blue circle is centered around a different point-source, representing a plane of constant phase of an elementary spherical wave for one wavelength λ. To record the resulting spectra on a screen located before (BW) or behind

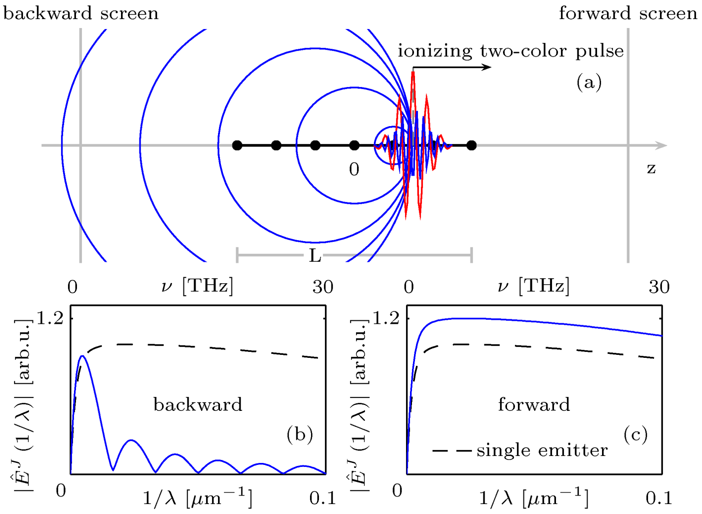

Figure 1: (a) Schematic illustration of the interference being responsible for shaping FW and BW emission. A plasma line-source of length L created by a propagating two-color pump pulse emits radiation. Blue circles centered around exemplary point-sources represent planes of constant phase of elementary spherical waves. In FW direction (c), spherical waves interfere constructively for all wavelengths and the resulting on-axis spectrum is proportional to the single emitter spectrum. In BW direction (b), the spectral form-factor Eq. (2) depletes wavelengths smaller than the source length (here $L = 30\ \mu$m).

(FW) the line, Jefimenkos's equation [8]

$$E^J\left(\vec{r},t\right) = -\frac{1}{4\pi\epsilon_0}\int\left(\frac{1}{c^2R}\frac{\partial J_e\left(\vec{r}',t-R/c\right)}{\partial t}\right)d^3\vec{r}' \tag{1}$$

is used to calculate the electric field emitted from a given current distribution. Here, $R = |\vec{r}-\vec{r}'|$ is the distance between the emitting point-source and the screen.

In this simplified situation, the FW on-axis spectrum is just proportional to the spectrum of a single point emitter $|\hat{E}_0^J(\lambda^{-1})|$, because contributions from emitters along the plasma line add up constructively for all wavelengths λ [see Fig. 1(c)]. In contrast, the BW on-axis spectrum differs significantly from the single emitter spectrum [see Fig. 1(b)], since radiation from different emitters is superposed with different temporal delays. The influence of these delays on the BW spectrum can be accounted for by a wavelength dependent form-factor

$$f(\lambda^{-1}) = \mathrm{Ei}\left[\frac{i4\pi}{\lambda}(z-L/2)\right] - \mathrm{Ei}\left[\frac{i4\pi}{\lambda}(z+L/2)\right], \tag{2}$$

which can be obtained from Eq. (1) by assuming a uniform current density being temporally shifted by z'/c along the line. Here, $\mathrm{Ei}(x) = \int_{-\infty}^{x}\frac{\exp(x')}{x'}dx'$ and z is the position of the screen. The on-axis BW spectrum is then proportional to $|f(\lambda^{-1})\hat{E}_0^J(\lambda^{-1})|$. Figure 1(b) reveals that the BW spectrum gets depleted for wavelengths $\lambda \ll L$, whereas it coincides with the FW spectrum for $\lambda \gg L$, because for these wavelengths the plasma line appears as a point source.

We now confront our predictions with rigorous two-dimensional (2D) Maxwell simulations, including plasma-induced propagation effects. We consider two-color input pump pulses

$$\begin{aligned} E_{\mathrm{in}}(r_\perp, t) = &\left[\sqrt{1-\xi}\cos\left(\omega_0 t\right) + \sqrt{\xi}\cos\left(2\omega_0 t + \varphi\right)\right] \\ &\times A \exp\left(-\frac{r_\perp^2}{w^2} - \frac{t^2}{\sigma_t^2}\right) \end{aligned} \tag{3}$$

with amplitude A, beam width w, pulse duration σ_t, $r_\perp = x$ (2D) or $r_\perp = \sqrt{x^2+y^2}$ (3D), ratio of fundamental ($\omega_0 = 2\pi\nu_0$, $\nu_0 = 375$ THz) and second harmonic ξ, relative phase φ, being focused into argon gas at atmospheric pressure. The density of generated free electrons obeys $\partial_t \rho_e = W_{\mathrm{ST}}(E)\left[\rho_{at} - \rho_e(t)\right]$, where ρ_{at} is the neutral atomic density and $W_{\mathrm{ST}}(E)$ a field dependent tunneling ionization rate [5,6]. We assume zero velocity for newly born electrons which are then accelerated in the electric field, leading to the current density [2, 5, 9]

$$\frac{\partial}{\partial t} J_e + \frac{1}{\tau_c} J_e = \frac{q^2}{m_e} E(t)\rho_e(t). \tag{4}$$

We model 2D transversal electric (TE) field evolution by means of the finite difference time domain (FDTD) method [10], solving Maxwell's equations

$$\begin{aligned} \mu_0 \frac{\partial H_x}{\partial t} =& \frac{\partial E_y}{\partial z}, \quad -\mu_0 \frac{\partial H_z}{\partial t} = \frac{\partial E_y}{\partial x}, \\ \frac{\partial D_y}{\partial t} + J_e =& \frac{\partial H_x}{\partial z} - \frac{\partial H_z}{\partial x}. \end{aligned} \tag{5}$$

Linear dispersion of argon is included via $\hat{D}_y(\omega) = \epsilon_0 n^2(\omega)\hat{E}_y(\omega)$, with the refractive index $n(\omega)$ given in [11]. In all FDTD calculations we neglect Kerr nonlinearities, because they play a minor role for THz generation in the present configuration. Figure 2 shows results for a focused ($f = 125$ μm) pump pulse with $A = 13.6$ GV/m, $w = 32$ μm, $\sigma_t = 34$ fs, $\xi = 0.2$, and $\varphi = \pi/2$. In excellent agreement with our theoretical predictions, the BW spectrum [Fig. 2(a)] is very narrow compared to the FW one [Fig. 2(b)]. Moreover, estimating the length $L \simeq 30$ μm of the plasma channel [Fig. 2(d)] and evaluating Eq. (2) leads to a BW spectral $1/e$-width of $\Delta\nu = 5$ THz, which coincides with the numerical obtained one at $z = -60$ μm. The ratio of on-axis BW and FW THz field amplitudes in Fig. 2(d) is about 0.1. To further validate the interference to be the governing effect shaping the BW spectrum, we linearly propagate a two-color Gaussian pump pulse in 3D geometry and use Jefimenko's Eq. (1) to compute the BW spectrum (3D Jefimenko approach). In order to get a comparable plasma channel, we adjust initial width and amplitude to $w = 25$ μm and $A = 6$ GV/m compared to the previous 2D configuration. The inset in Fig. 2(a) shows the resulting BW spectrum, reproducing again the predicted and simulated spectral width of 5 THz.

In the simple picture developed in Fig. 1 and Eqs. (1), (2) we ignore the opacity of the generated plasma for frequencies below the plasma frequency $2\pi\nu_p = \sqrt{\rho_e q^2/\epsilon_0 m_e}$. In the 2D examples above we find $\nu_p \approx 45$ THz, but the generated plasma channel is small in transverse direction [≈ 3 μm, see Fig. 2(d)] and THz radiation strongly diffracts, so we find our spectra still governed by the predicted interference effects. To check the influence of broader plasma channels, we confine our setup to the extreme case of one dimension (1D), neglecting all transverse spatial

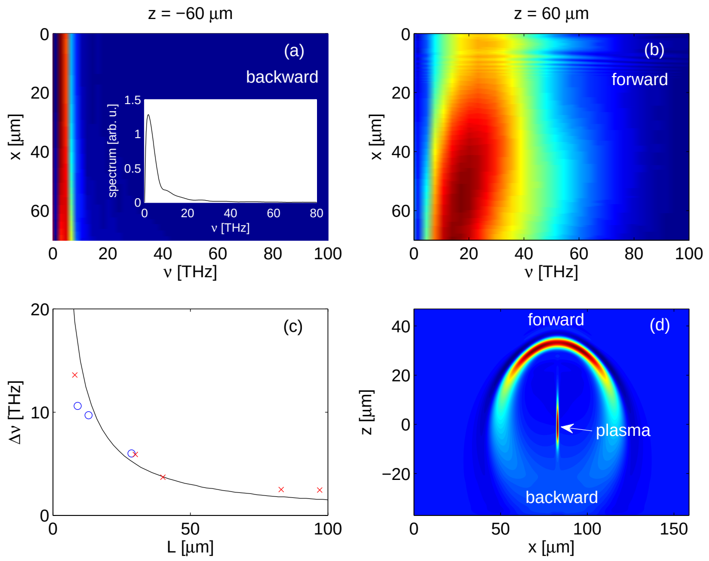

Figure 2: 2D FDTD simulations: THz spectra of (a) BW and (b) FW emission. The inset shows the on-axis BW spectrum obtained from a linearly propagated Gaussian pump pulse and Eq. (1). (c) On-axis BW spectral width vs. plasma channel length L from Eq. (2) (solid line), 2D FDTD calculations (blue circles), and 3D Jefimenko approach (red crosses). (d) Snapshot of emitted THz fields (< 100 THz) and plasma channel, illustrating the strong (weak) emission in FW (BW) direction.

dependencies. Two-color pump pulses are launched in vacuum and hit a 1 mm thick argon layer. This setup enables us to record BW spectra in FDTD simulations. For additional comparison, we simulate the FW fields by using a unidirectional pulse propagation equation (UPPE) [12]. This approach describes pump as well as the emitted THz fields in FW direction and was shown to reproduce experimental results [6]. In our UPPE code, we can also include third order nonlinear polarization (Kerr effect), which is neglected in the FDTD simulations. The UPPE approach does not account for plasma opacity, whereas it is naturally included in the FDTD simulations. Figure 3 shows pump pulses with $\sigma_t = 34$ fs, $\xi = 0.2$, and $\varphi = \pi/2$ and amplitudes $A = 31$ GV/m and 46 GV/m launched into argon at pressure $p = 1$ bar ($\rho_{at} = 2.7 \times 10^{25}$ m^{-3}) and $p = 5$ bar ($\rho_{at} = 13.5 \times 10^{25}$ m^{-3}), respectively. The generated plasma is opaque for frequencies below $\nu_p = 22$ THz ($A = 31$ GV/m, $\rho_e^{\max} = 6 \times 10^{24}$ m^{-3}) and $\nu_p = 104$ THz ($A = 46$ GV/m, $\rho_e^{\max} = 13.5 \times 10^{25}$ m^{-3}). For the FW emitted THz radiation the opacity of the plasma plays almost no role, we obtain excellent agreement between FDTD and UPPE simulations [see Fig. 3(a,b)]. The reason is that the THz field is emitted before the plasma builds up [Fig. 3(c)], thus no damping influences its further FW propagation. In contrast, in BW direction plasma-opacity is important and only frequencies $\nu > \nu_p$ propagate through the already built up plasma. Therefore, in 1D geometry Eq. (2) is applicable only for $\nu > \nu_p$, and for a plasma length of 1 mm entirely destructive interference is expected. Indeed, this can be seen from the cutoffs of the BW spectra at the corresponding plasma frequencies in Fig. 3(d). Below these frequencies ν_p, radiation originates from the front-side of the plasma layer only, since contributions from deeper inside are damped.

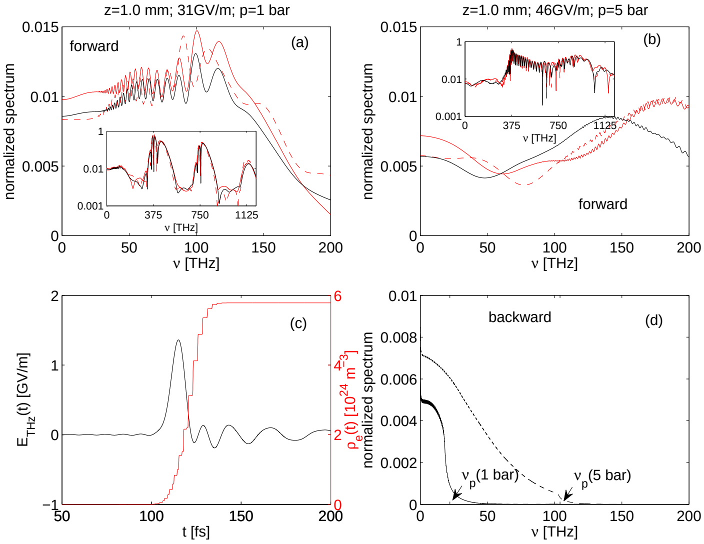

Figure 3: 1D simulations: FW THz spectra for (a) $A = 31$ GV/m (1 bar) and (b) $A = 46$ GV/m (5 bar) from FDTD (black line) and UPPE simulations with (dashed red line) and without (solid red line) Kerr effect included. The insets show the complete spectra. (c) UPPE results illustrate that THz emission (black line) takes place mainly at the ionization front (red line). (d) BW THz spectra for parameters used in (a) (solid line) and (b) (dashed line), both obtained from FDTD simulations. All spectra are normalized to $|\hat{E}_{\text{in}}\,(\nu = 375\ \text{THz})|$.

In conclusion, we explained the differences in FW and BW emitted THz spectra from gas plasmas observed in full Maxwell numerical simulations by simple interference effects. Forward spectra are well described by unidirectional models and opacity of the plasma has negligible influence. We believe that the predicted sensitivity of the BW THz spectral width on the length of the plasma channel could be tested experimentally in a straight-forward manner.

This work was performed using HPC resources at Rechenzentrum Garching and from GENCI-CCRT (Grant 2010-x2010106003). I. B. acknowledges support by the DFG and E. CG. from FIS2009-07870.

References

[1] D. J. Cook and R. M. Hochstrasser, Opt. Lett. **25**, 1210 (2000).

[2] K.-Y. Kim, J. H. Glownia, A. J. Taylor, and G. Rodriguez, Opt. Express **15**, 4577 (2007).

[3] T. Bartel, P. Gaal, K. Reimann, M. Woerner, and T. Elsaesser, Opt. Lett. **30**, 2805 (2005).

[4] J. Dai, X. Xie, and X.-C. Zhang, Phys. Rev. Lett. **97**, 103903 (2006).

[5] M. D. Thomson M. Kreß, T. Löffler, and H. G. Roskos, Laser & Photon. Rev. **1**, 349 (2007).

[6] I. Babushkin, W. Kuehn, C. Köhler, S. Skupin, L. Bergé, K. Reimann, M. Woerner, J. Herrmann, and T. Elsaesser, Phys. Rev. Lett. **105**, 053903 (2010).

[7] J. Peñano, P. Sprangle, B. Hafizi, D. Gordon, P. Serafim, Phys. Rev. E **81**,026407 (2010).

[8] O. D. Jefimenko, *Electricity and Magnetism: An Introduction to the Theory of Electric and Magnetic Fields* (Appleton-Century-Crofts, New-York, 1966).

[9] I. Babushkin, S. Skupin, and J. Herrmann, Opt. Express **18**, 9658 (2010).

[10] R. M. Joseph and A. Taflove, IEEE Trans. Antenna Propagat. **45**, 364 (1997).

[11] A. Dalgarno and A. E. Kingston, Proc. Roy. Soc. London A **259**, 424 (1960).

[12] M. Kolesik and J. V. Moloney, Phys. Rev. E **70**, 036604 (2004).